

The 28 GeV Dimuon Excess in Lepton Specific 2HDM

Ali Çiçi^{a1}, Shaaban Khalil^{b2}, Büşra Niş^{a3} and Cem Salih Ün^{a4}

^a*Department of Physics, Bursa Uludağ University, TR16059 Bursa, Turkey*

^b*Center of Fundamental Physics, Zewail City of Science and Technology, Sheikh Zayed, 12588 Giza, Egypt*

Abstract

We explore the Higgs mass spectrum in a class of Two Higgs Doublet Models (2HDMs) in which a scalar $SU(2)_L$ doublet interacts only with quarks, while the second one interacts only with leptons. The spectrum includes two CP-even Higgs bosons, either of which can account for the SM-like Higgs boson, in addition light scalars (CP-even or -odd) can be accommodated. When the lightest CP-even scalar (h_1) is assigned to be the SM-like Higgs boson, the heavier CP-even (h_2) and charged Higgs bosons (H^\pm) become above 600 GeV. If h_2 is required to satisfy the SM-like Higgs boson constraints, then h_1 can be lighter than 50 GeV and can count for a possible state leading to an excess in dimuon processes. Also, in case of light pseudo scalar, $m_A \lesssim 50$ GeV, an excess in dimuon invariant mass can be accommodated in this class of models through A -boson production in association with a b -jet.

¹E-mail: 501507007@ogr.uludag.edu.tr

²E-mail: skhalil@zewailcity.edu.eg

³Email: 501507008@ogr.uludag.edu.tr

⁴E-mail: cemsalihun@uludag.edu.tr

1 Introduction

Since it was observed in 2012 [1], the analyses have been precisely performed on the 125 GeV Higgs boson, and they resulted in the fact that the Standard Model predictions are mostly consistent with the experimental observations. The decay modes of the Higgs boson to $\gamma\gamma$, ZZ (ended with $4l$), and WW have led to quite precise measurements of the mass and production of the Higgs boson [2]. Even though some excesses were reported [3], the thorough analyses have shown that the SM predictions are in a good agreement with the experimental observations, especially for $h \rightarrow \gamma\gamma$ and $h \rightarrow 4l$ decay channels [4].

The richness in the decay modes of the Higgs boson allows to combine the results and lead to the possible highest precision in analyses [5]. Apart from the uncertainties [6], some deviations are also reported from analyses such as Higgs boson production in association with W or Z boson and $h \rightarrow b\bar{b}$ measurements [7]. While the analyses can severely constrain, such deviations can provide a window for new physics (NP). Besides, these analyses are also performed for the mass scales other than 125 GeV [8] in order to probe the probability for the existence of extra Higgs bosons, whose observations would be interpreted as a direct signal for NP, and could probe the models beyond the SM. For instance, recent analyses have reported an excess at about 28 GeV in the mass spectrum of the muon pairs detected in the collider experiments [9].

A similar excess at about 30 GeV was indicated also by the ALEPH data, which was revealed in the analyses of $Z \rightarrow b\bar{b}\mu^+\mu^-$ [10]. One can relate the results from these analyses to the recent ones represented in [9], since the state leading to the excess is in association with b -jets. This excess can be provided by either a scalar or vector boson [11], but in any case it requires a new state, which is not included in the SM. If the excess is caused by a neutral scalar state, such a state can be accommodated in the models which have at least two Higgs doublets. In this context the most economical way is to extend the SM by one more Higgs doublet, which forms the class of Two Higgs Doublet Models (2HDMs). Adding one additional Higgs doublet enriches the Higgs sector such that the spectrum involves two CP-even Higgs bosons, a CP-odd Higgs boson and two charged Higgs bosons [12]. Even though the most studies assign the lightest CP-even Higgs boson to the SM-like Higgs boson, in principal, the heaviest CP-even Higgs boson can be treated as the SM-like Higgs boson as well. One of the salient features of 2HDMs is that one can realize light CP-odd Higgs boson consistent with the current experimental results [13, 14].

In this context, if a CP-odd Higgs boson can be realized as light as about 30 GeV, it can be also a viable candidate for the state which leads to the excess in the mass of the muon pair. However, a problem with the light scalar states can arise from the rare B -meson decays such as $B_s \rightarrow \mu^+\mu^-$ and $B_s \rightarrow X_s\gamma$, where X_s denotes a meson with a strange quark. These processes receive contributions from the scalar states [15], and the agreement between the SM predictions [16] and the experimental measurements [17] yields a strong impact on the low scale predictions.

In our study, we assume the dimuon excess arises from the presence of a scalar state. We explore the mass spectrum of the Higgs boson in a class of 2HDMs, in which the Higgs doublets distinguish the leptons such that one of them interacts only with leptons, while the other does not at tree-level. This class of models is called Lepton Specific 2HDM (LS-2HDM), and it can be realized by imposing a Z_2 symmetry as well as CP conservation. Several Z_2 symmetries can be necessary in 2HDM to restrict the Yukawa interactions in order to prevent flavor changing neutral currents [18].

The paper is organized as follows. In Section 2 we first briefly describe the LS-2HDM and its Higgs sector. Our results for the Higgs mass spectrum consistent with several experimental constraints are Section 3. In Section 4, we consider a case in which the CP-odd Higgs boson of mass about 28 GeV can yield an excess in dimuon mass distribution, while we also consider the possibility for a CP-even Higgs boson leading to excess in Section ???. In these sections, we consider possible signal processes in which a light Higgs boson is produced in association with $b\bar{b}$, follow a similar analysis represented in [9]. Finally we conclude in Section 5.

2 Lepton Specific 2HDM

Even though the SM has only one Higgs doublet, its symmetrical structure does not prevent to have more Higgs doublets in its content. In spite of its great success, there are still theoretical and experimental motivations to extend its scalar sector such as spontaneous CP-violation [19], the CP violation in the strong sector [20], baryogenesis [21] etc. In addition, the models with two Higgs doublets can accommodate light Higgs bosons in the mass spectrum. In this case, one of the strongest impact may come from the rare B -meson decays. The process $B_s \rightarrow \mu^+\mu^-$ receives contributions from the CP-odd Higgs boson (A) exchange, which is, in general, proportional to $(\tan\beta)^6/m_A^4$ [22]. A light A -boson can overcontribute to this process and it can spoil the quite good agreement between the SM [23] and the experimental measurements [17]. If the charged Higgs boson is realized nearly degenerate to A -boson, then also the process $B_s \rightarrow X_s\gamma$ predictions become problematic. However, despite strong impacts from these processes, it might still be possible to realize light Higgs bosons in the spectrum.

The rich vacuum structure of 2HDMs also allows to accommodate some implications such as lepton flavor violation or flavor changing neutral currents. The severe constraints on the tree-level lepton flavor violation strongly restricts the Yukawa couplings between the charged leptons and the Higgs bosons. In addition, the absence of the flavor changing neutral currents can be satisfied by imposing a Z_2 symmetry, and different Z_2 symmetries lead to different types of 2HDMs. We choose to impose a Z_2 symmetry such that $\Phi_1 \rightarrow -\Phi_1$, $\Phi_2 \rightarrow \Phi_2$ and $e_R \rightarrow -e_R$ is applied to the scalar potential and Yukawa Lagrangian in the 2HDM framework, where Φ_i are the scalar fields, while e_R denotes the right-handed charged lepton. Assuming all other fields are even under this Z_2 symmetry leads to a Yukawa Lagrangian such that quarks interact only with Φ_2 , while leptons have a vertex only with Φ_1 as follows:

$$\mathcal{L}_Y = -Y^u \bar{Q}_L \tilde{\Phi}_2 u_R + Y^d \bar{Q}_L \Phi_2 d_R + Y^e \bar{L} \Phi_1 e_R, \quad (1)$$

where Q and L stand for the left-handed quark and lepton doublets, while u_R , d_R and e_R are the right-handed $SU(2)$ singlet quark and lepton fields respectively. This class of THDM models refer to LS-2HDM. We have suppressed the family indices for simplicity, and $\tilde{\Phi}_2 = i\sigma_2\Phi_2$.

Y_u^h	Y_d^h	Y_l^h	Y_u^H	Y_d^H	Y_l^H	Y_u^A	Y_d^A	Y_l^A
$\cos\alpha/\sin\beta$	$\cos\alpha/\sin\beta$	$-\sin\alpha/\cos\beta$	$\sin\alpha/\sin\beta$	$\sin\alpha/\sin\beta$	$\cos\alpha/\cos\beta$	$\cot\beta$	$-\cot\beta$	$\tan\beta$

Table 1: Effective Yukawa couplings between the quarks, leptons and the Higgs bosons.

In the LS-2HDM framework, if the light Higgs bosons are formed mostly by the fields in Φ_1 , then their interactions with the quarks become proportional to $\cot \beta$, and their contributions are suppressed, if $\tan \beta$ is large. If the lightest CP-even Higgs boson is required to be the SM-like Higgs boson, then the consistent solutions yield the SM-like Higgs boson mostly formed by Φ_2 . This is because the top quark receives its large tree-level mass from vacuum expectation values (VEVs) of the fields in Φ_2 , and the relevant Yukawa couplings cannot compensate small VEVs in Φ_2 due to the perturbativity condition. Thus, one can conclude that consistent solutions are more likely yield the SM-like Higgs boson mostly formed by the fields of Φ_2 doublet. In this case, A -boson couples to the matter fields inversely proportional to $\tan \beta \equiv v_2/v_1$, where $v_{1,2}$ are the VEVs of $\Phi_{1,2}$. Table 1 summarizes the couplings of the Higgs bosons to the matter fields.

Imposing CP-conservation, the invariance under the Z_2 symmetry significantly simplifies the most general Higgs potential. However, the perturbativity constraint on the scalar potential requires a soft term which breaks Z_2 [24]. In this context, the scalar potential can be given as

$$V(\Phi_1, \Phi_2) = m_1^2 \Phi_1^\dagger \Phi_1 + m_2^2 \Phi_2^\dagger \Phi_2 + m_3^2 (\Phi_1^\dagger \Phi_2 + \Phi_2^\dagger \Phi_1) + \frac{1}{2} \lambda_1 (\Phi_1^\dagger \Phi_1)^2 + \frac{1}{2} \lambda_2 (\Phi_2^\dagger \Phi_2)^2 + \lambda_3 (\Phi_1^\dagger \Phi_1) (\Phi_2^\dagger \Phi_2) + [\frac{1}{2} \lambda_5 (\Phi_1^\dagger \Phi_2)^2 + \text{h.c.}] , \quad (2)$$

where $m_{1,2,3}$ are the mass terms for the Higgs doublets, and λ_i stand for the couplings between the Higgs fields. In writing the scalar potential above we follow the general notation in [25], where $\lambda_{4,6,7,8,9,10}$ are required to be zero by the invariance under the charge conjugation, and Z_2 symmetry mentioned in the beginning of this section. Note that the term with m_3 softly breaks the Z_2 symmetry as well as mixing the Higgs fields together with λ_3 and λ_5 . The physical spectrum, as is well known, includes two CP-even and one CP-odd neutral Higgs bosons, as well as two charged Higgs bosons. These physical states can be obtained by rotating the mixing parameters away by field redefinitions. Defining $\tan \beta \equiv v_2/v_1$ and $v^2 = v_1^2 + v_2^2$, the tree-level mass-squared matrix for the CP-even Higgs fields can be obtained as follows:

$$\mathcal{M}^2 = \begin{pmatrix} m_3^2 \tan \beta - \lambda_5 v^2 \sin^2 \beta + \lambda_1 v^2 \cos^2 \beta & -m_3^2 - \lambda_5 \sin \beta \cos \beta + \lambda_3 v^2 \sin \beta \cos \beta \\ -m_3^2 - \lambda_5 \sin \beta \cos \beta + \lambda_3 v^2 \sin \beta \cos \beta & m_3^2 \cot \beta - \lambda_5 v^2 \cos^2 \beta + \lambda_2 v^2 \sin^2 \beta \end{pmatrix} \quad (3)$$

Note that $m_{1,2}^2$ are eliminated by using the tadpole equations. The tree-level masses of the physical CP-even neutral Higgs bosons are simply the eigenvalues of the mass squared matrix given in Eq.(3). Instead of writing down the Higgs boson masses in terms of the scalar potential parameters, one can relate the Higgs boson masses to each other by choosing one the Higgs boson mass, say the CP-odd Higgs boson mass m_A , which is obtained at tree-level, which is

$$m_A^2 = \frac{m_3^2}{\sin \beta \cos \beta} - \lambda_5 v^2 , \quad (4)$$

and using its mass expression the other Higgs boson masses can be written as follows [24]:

$$\begin{aligned}
m_{h_1}^2 &= m_A^2 \cos^2(\beta - \alpha) + v^2 \left[\lambda_1 \cos^2 \beta \sin^2 \alpha + \lambda_2 \sin^2 \beta \cos^2 \alpha \right. \\
&\quad \left. - \frac{1}{2} \lambda_3 \sin(\beta + \alpha) + \lambda_5 \cos^2(\beta - \alpha) \right] , \\
m_{h_2}^2 &= m_A^2 \sin^2(\beta - \alpha) + v^2 \left[\lambda_1 \cos^2 \beta \cos^2 \alpha + \lambda_2 \sin^2 \beta \sin^2 \alpha \right. \\
&\quad \left. + \frac{1}{2} \lambda_3 \sin(\beta + \alpha) + \lambda_5 \sin^2(\beta - \alpha) \right] , \\
m_{H^\pm}^2 &= m_A^2 + \frac{1}{2} \lambda_5 v^2
\end{aligned} \tag{5}$$

where h_1 and h_2 represent the lightest and heaviest CP-even Higgs boson states, and α stands for the mixing angle of the CP-even Higgs fields. Note that one these CP-even Higgs bosons should exhibit the SM-like Higgs boson properties. These relations can be discussed in terms of the VEVs of the Higgs fields and their mixing angle. As is discussed above, consistent solutions need $v_2 > v_1$. When $\tan \beta$ is large or moderate, the constraint from the 125 GeV Higgs boson observations can be satisfied either by large λ_3 (~ 1), or significant mixing in the CP-even Higgs sector ($\sin \alpha \sim \mathcal{O}(1)$). Such a mixing can be realized with large or moderate values of m_3^2 , which yields $m_A \gg m_h$ according to Eq.(4).

On the other hand, our discussion over the masses and mixing in the Higgs sector is based on the tree-level masses. However, the loop contributions must count in the mass calculations, since those, especially from the third family matter fields, can significantly contribute to tree-level masses of the Higgs bosons. In this case, the the tension from the SM-like Higgs boson constraints can be loosen. Indeed, a recent study [14] has shown that light Higgs bosons can be accommodated in the spectrum consistent with the current experimental results, and A -boson can be realized as light as about 50 GeV. However, the suppression in the coupling between A -boson and the quarks will also yield a suppression in the A -boson production in the colliders. In this context, realizing consistently light A -boson does not mean easy detection in the experiments. A similar discussion can be followed for the charged Higgs boson (H^\pm) under the constraints from the $B_s \rightarrow X_s \gamma$ process. However, LEP II results have model independently excluded the presence of any charged state lighter than about 80 GeV [26]. In this context, we will focus on the mass spectrum and the production rates of the light Higgs bosons, and we refer to Ref. [25], for more detailed reviews and other salient features of 2HDMs.

3 Higgs Mass Spectrum and Production at LHC

We display our results for the mass spectrum of the Higgs bosons, which are calculated by varying m_3 , $\tan \beta$ and λ_i ($i = 1, 2, 3, 5$) defined in Eq.(2). Note that m_1^2 and m_2^2 are calculated by minimalizing the scalar potential. In generating the mass spectrum we use SPheno-4.0.3 package [27, 28] generated with SARAH 4.13.0 [29, 30]. Scanning over these parameters, we allow only solutions which are consistent with the electroweak symmetry breaking ($v^2 = v_1^2 + v_2^2 \simeq v_{\text{SM}}^2$, where v_{SM} is the VEV of the SM Higgs boson.), and the observed fermion masses. After collecting the data we successively apply the constraints from the Higgs boson masses and the rare B -meson decays as follows:

$$\begin{aligned}
123 \leq m_{h_i} &\leq 127 \text{ GeV} , \\
m_{H^\pm} &\gtrsim 80 \text{ GeV} , \\
0.8 \times 10^{-9} \leq \text{BR}(B_s \rightarrow \mu^+ \mu^-) &\leq 6.2 \times 10^{-9} (2\sigma) , \\
2.99 \times 10^{-4} \leq \text{BR}(b \rightarrow s \gamma) &\leq 3.87 \times 10^{-4} (2\sigma) .
\end{aligned} \tag{6}$$

where m_{h_i} stand for the CP-even Higgs bosons with $i = 1, 2$.

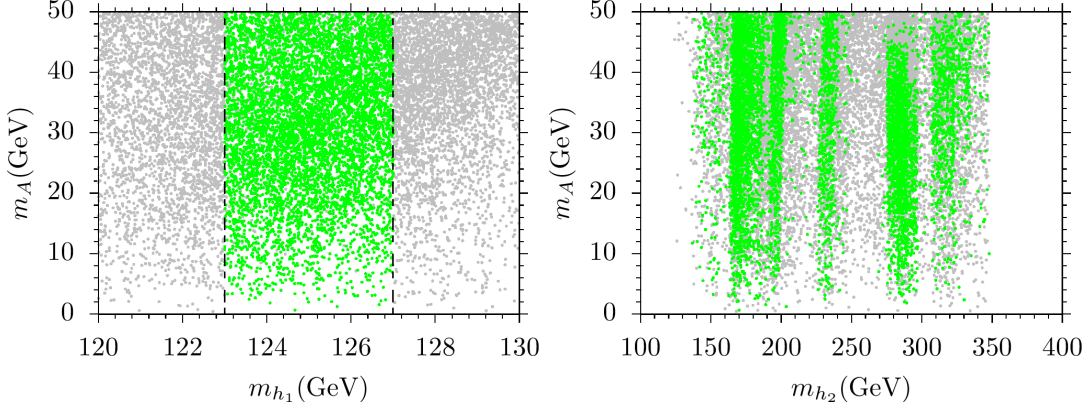


Figure 1: Plots in the $m_A - m_{h_1}$ and $m_A - m_{h_2}$ planes. All points are consistent with the electroweak symmetry breaking and observed fermion masses. Green points are consistent with the constraints from rare B -meson decays and the Higgs boson masses as $123 \leq m_{h_1} \leq 127$ GeV, and $m_{H^\pm} \gtrsim 80$ GeV.

We first consider the solutions in which the lightest CP-even Higgs boson (h_1) is required to satisfy the SM-like Higgs boson properties, while the A -boson are allowed to be as light as about $\mathcal{O}(10)$ GeV. Figure 1 displays the Higgs boson mass spectrum with plots in the $m_A - m_{h_1}$ and $m_A - m_{h_2}$ planes. All points are consistent with the electroweak symmetry breaking and observed fermion masses. Green points are consistent with the constraints from rare B -meson decays and the Higgs boson masses as $123 \leq m_{h_1} \leq 127$ GeV, and $m_{H^\pm} \gtrsim 80$ GeV. Despite excluding a significant portion of the parameter space, as is seen from the $m_A - m_{h_1}$ plane, the constraint from the SM-like Higgs boson observations still allows solutions with $m_A \leq 50$ GeV consistent also with the constraints from the rare B -meson decays and charge Higgs boson mass. The region with light m_A also yields $m_{h_2} \lesssim 350$ GeV, as shown in the $m_A - m_{h_2}$ panel of Figure 1.

As mentioned before, in spite of being light, these Higgs bosons may not abundantly be produced in the collider experiments due to their couplings to quarks, which is inversely proportional to $\tan \beta$. The top panels of Figure 2 display the production of the CP-odd Higgs boson in correlation with its mass, when the lightest CP-even Higgs boson is assigned to be the SM-like. In the current LHC experiments with 14 TeV center of mass (COM) energy, $\sigma(pp \rightarrow A)$ can be as high as about 700 pb if its mass is of order about 10 GeV, and the cross-section reduces to about 400 pb when $m_A \sim 30$ GeV. One can expect its production cross-section to be quite high (~ 5000 pb) in the Future Circular Collider (FCC) experiments with 100 TeV COM energy, as seen from the top-right panel of Figure

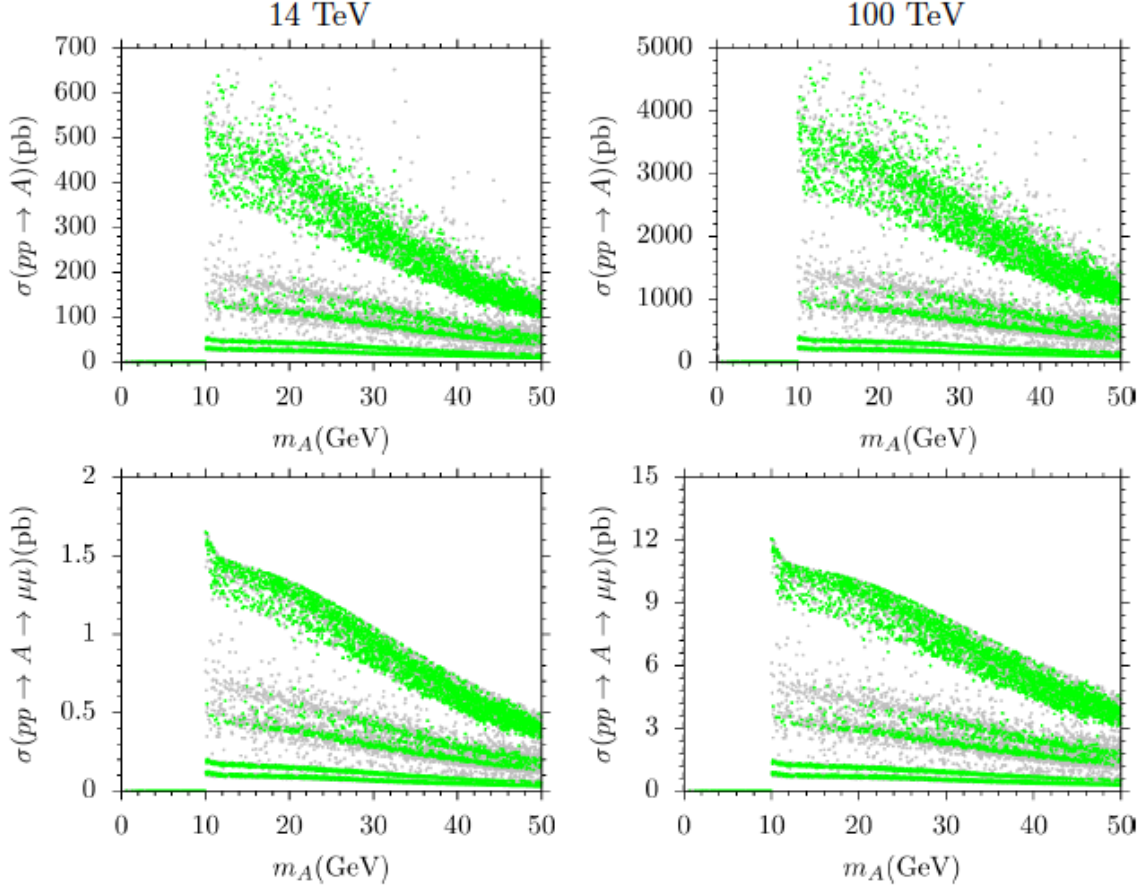


Figure 2: Top panels represent the CP-odd Higgs boson production in a correlation with its mass at the LHC (left) and FCC (right) experiments. Bottom panels display the approximate cross-section for the $pp \rightarrow A \rightarrow \mu\mu$ in correlation with its mass at the LHC (left) and FCC (right) experiments. The color coding is the same as in Figure 1.

2. If one follows the following approximation¹ for the cross-section of entire process

$$\sigma(pp \rightarrow A \rightarrow \mu^+ \mu^-) \approx \sigma(pp \rightarrow A) \times \text{BR}(A \rightarrow \mu^+ \mu^-) , \quad (7)$$

the results are found as represented in the bottom panels of Figure 2. At the current LHC experiment, the signal can be expected at about 1.5 pb, while FCC experiments can detect this process at about 10 pb.

In principal, one can also consider the solutions in which the heaviest CP-even Higgs boson (h_2) is required to satisfy the SM-like Higgs boson properties. In this case, h_1 is allowed to be much lighter unless the experimental constraints are not violated. Figure 3 represents the mass spectrum for such cases. As is seen from the $m_A - m_{h_2}$ plane, A -boson is mostly heavier than about 150 GeV, even though it can also be realized at about 30 GeV consistently. The mass spectrum, in this case, involves the lightest CP-even Higgs boson as light as about a few GeV.

We proceed with the production of light CP-even Higgs boson shown in Figure 4 in a

¹Comparing this approximation with full MadGraph calculation yields an error of order about 1% at most [34].

correlation with its mass at the LHC (left) and FCC (right) experiments. Bottom panels are the approximate cross-section for the $h_1 \rightarrow \mu\mu$ in correlation with its mass at the LHC

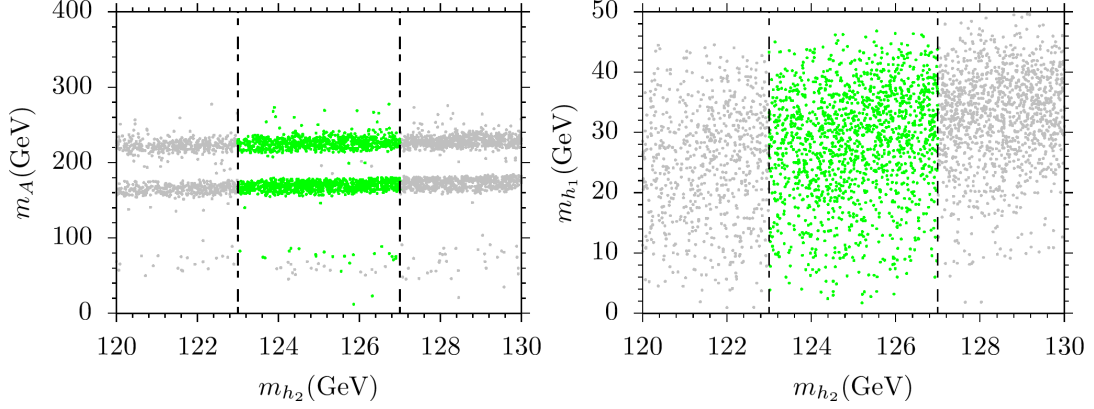


Figure 3: Plots in the $m_A - m_{h_2}$ and $m_{h_1} - m_{h_2}$ planes. All points are consistent with the electroweak symmetry breaking and observed fermion masses. Green points are consistent with the constraints from rare B -meson decays and the Higgs bosons as $123 \leq m_{h_2} \leq 127$ GeV and $m_{H^\pm} \gtrsim 80$ GeV.

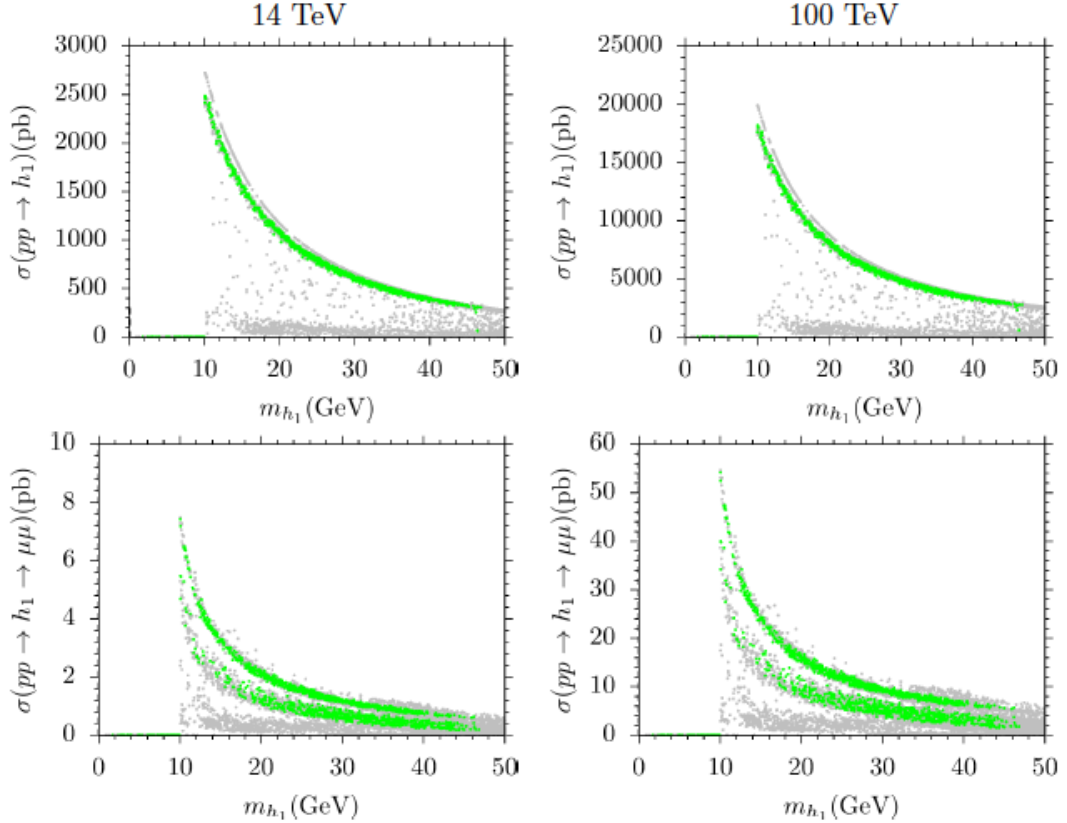


Figure 4: Top panels represent the lightest CP-even Higgs boson production in a correlation with its mass at the LHC (left) and FCC (right) experiments. Bottom panels are the approximate cross-section for the $h_1 \rightarrow \mu\mu$ in correlation with its mass at the LHC (left) and FCC (right) experiments. The color coding is the same as in Figure 3.

(left) and FCC (right) experiments. The color coding is the same as in Figure 3. As seen from the top-left panel, even in the current experiments at the LHC, its production can be realized as high as about 1000 pb when $m_{h_1} \sim 30$ GeV, while it is expected to be about eight times larger (~ 8000 pb) in the FCC experiments as shown in the top-right panel of Figure 4. Thus, the signal process is also expected to be large proportionally. The bottom panels of Figure 4 shows that the current LHC experiments can probe the process at about $\sigma(pp \rightarrow h_1 \rightarrow \mu^+\mu^-) \sim 2$ pb, and it can be realized at about 14 pb in the FCC experiments.

4 Dimuon Resonance

We have discussed the mass spectrum of the Higgs bosons in the previous section, and we have seen that it is possible to realize light Higgs bosons consistent with the experimental constraints, and the solutions yield a considerable amount of production of them. In this section, we exemplify our findings with two benchmark points given in Table 2. The points are chosen as to yield the greatest production cross-sections when $m_A \simeq 28$ GeV (Point 1), or $m_{h_1} \simeq 28$ GeV (Point 2). All masses are given in GeV, and cross-sections in pb. Note that the electroweak symmetry breaking requires $m_i^2 < 0$. The hyphens in $\sigma(A \rightarrow \mu^+\mu^-)$ of Point 1 and $\sigma(h_1 \rightarrow \mu^+\mu^-)$ of Point 2 mean the branching ratios of the considered decay modes are lower than about 10^{-5} .

	Point 1	Point 2
λ_1	0.67	0.24
λ_2	0.26	0.02
λ_3	0.54	-0.43
λ_4	-0.82	0.08
λ_5	0.15	-0.26
m_1	85.2	55.2
m_2	111.5	33.4
m_3	313.6	1376
m_{h_1}	125.3	27.3
m_{h_2}	178.6	123.4
m_A	27.9	168.2
m_{H^\pm}	173.8	134.4
$B_s \rightarrow \mu^+\mu^-$	0.33×10^{-8}	0.39×10^{-8}
$B_s \rightarrow X_s \gamma$	3.15×10^{-4}	3.15×10^{-4}
$\sigma(pp \rightarrow A)$	390.9	5.23
$\sigma(pp \rightarrow h_1)$	22.01	694
$\sigma(A \rightarrow \mu^+\mu^-)$	1.1	-
$\sigma(h_1 \rightarrow \mu^+\mu^-)$	-	1.42

Table 2: Benchmark points representing the Higgs boson mass spectrum. All masses are given in GeV, and cross-sections in pb. Point 1 depicts a solution with $m_A \sim 28$ GeV with $m_{h_1} \sim 125$ GeV, while Point 2 displays a solution with $m_{h_1} \sim 28$ GeV with m_{h_2} being the SM-like Higgs boson.

Employing MadGraph [31], we follow similar analyses represented in [9], in which a

light Higgs boson is produced in association with a b -jet, then it subsequently decays into a pair of muons. We first consider the signal process $pp \rightarrow b\bar{b}A \rightarrow b\bar{b}\mu^+\mu^-$, then we also discuss the case in which A -boson is replaced with the lightest CP-even Higgs boson, i.e. $pp \rightarrow b\bar{b}h \rightarrow b\bar{b}\mu^+\mu^-$. The main background is formed by the Drell-Yan, top pair production, single top quark processes. Also the the processes involving a $W^\pm + \text{jets}$ or diboson priduction can be listed; however, these processes are reported rather to be negligible [9].

Moreover, the optimization of the signal yields the following cuts on the signal and background processes:

- $p_T^{\mu_1} \gtrsim 25 \text{ GeV}$, $|\eta_{\mu_1}| < 2.1$; $p_T^{\mu_2} \gtrsim 5 \text{ GeV}$, $|\eta_{\mu_2}| < 2.4$,
- $p_T^{b\text{-jet}} \gtrsim 20 \text{ GeV}$, $|\eta_{\mu_1}| < 2.4$; $p_T^{\text{miss}} \lesssim 40 \text{ GeV}$

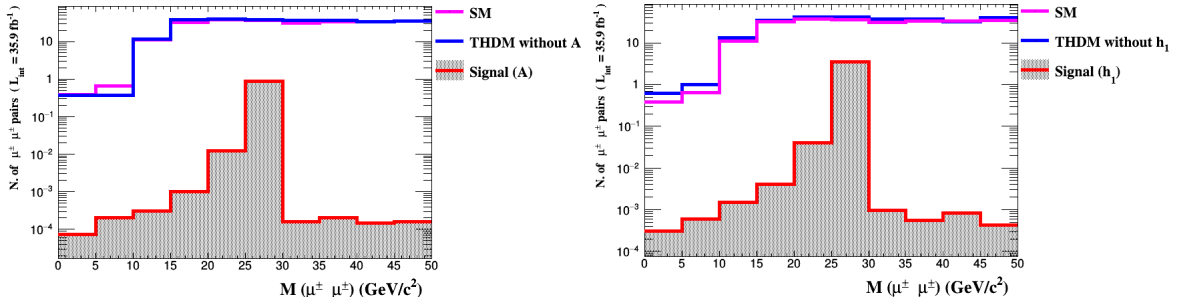


Figure 5: Collider analyses for Point 1 (left) and Point 2 (right). Magenta curve represents the total SM background, while blue displays the LS-THDM prediction without light Higgs bosons. The signal is depicted by the red curve for the CP-odd (left) and CP-even (right) Higgs bosons.

We show the comparison of LS-THDM and SM in Figure 5 for Point 1 (left) and Point 2 (right). Magenta curve represents the total SM background, while blue displays the LS-THDM prediction without light Higgs bosons. The signal is depicted by the red curve for the CP-odd (left) and CP-even (right) Higgs bosons. The total SM backgrounds (magenta) is obtained by summing over the relevant background processes mentioned above. The same processes are calculated in the LS-THDM framework (blue), and is seen from the both panels of Figure 5, the LS-THDM predictions mostly overlap with the SM, when the contributions from the Higgs bosons are left out. In this context, if a light A -boson can be accommodated in the spectrum, then its decay into a muon pair can be account for the excess in the observed invariant mass of the muon pair, as is shown in the right panel of Figure 5. Similar analyses can be performed when a CP-even Higgs boson (h_1) is as light as about 28 GeV depicted in Point 2. The left panel of Figure 5 shows that Point 2 also yields the similar predictions as the SM, when the $h_1 \rightarrow \mu^+\mu^-$ is not included in the dimuon processes, and the signal $pp \rightarrow b\bar{b}h_1 \rightarrow b\bar{b}\mu^+\mu^-$ can yield an excess at about 28 GeV in the invariant mass of the muon pair.

5 Conclusion

We consider the Higgs boson mass spectrum in the LS-2HDM framework. When the lightest CP-even Higgs boson is required to satisfy the 125 GeV Higgs boson observations

along with the constraints from the rare B -meson decays and charged Higgs boson mass, we find that h_2 can be as heavy as about 600 GeV, while the CP-odd Higgs boson can be much lighter as $m_A \lesssim 50$ GeV consistent with the experimental constraints. The parameter region with $m_A \sim 30$ GeV bounds h_2 mass further as $m_{h_2} \lesssim 350$ GeV. m_{h_2} is also bounded by the experimental constraints at about 150 GeV from below. One can also consider h_2 as a SM-like Higgs boson, and in this case the Higgs bosons are mostly found to be heavier than about 100 GeV, while the lightest CP-even Higgs boson can now be as light as about 28 GeV. Even though it also suppresses the production of these light Higgs bosons in collider experiments, we find $\sigma(pp \rightarrow A) \simeq 500$ pb at 14 TeV when $m_A \simeq 30$ GeV. Its production cross-section can be expected to enhance up to about 5000 pb, when FCC with 100 TeV starts operating. Under these circumstances, the approximate cross-section of $A \rightarrow \mu^+\mu^-$ process can be observed at the current LHC experiments at about rate of 1 pb, while FCC may observe it at about 10 pb. When the lightest CP-even Higgs boson is realized as light as about 28 GeV in the mass spectrum, its production can be realized much higher ($\sigma(pp \rightarrow h_1) \simeq 1000$ pb) in comparison with the case of light A -boson. Its production rare can be expected to raise up to about 8000 pb in the experiments conducted at FCC of 100 TeV.

We display two benchmark points exemplifying our findings. Point 1 is for the case with $m_A \sim 28$ GeV in which h_1 is adjusted to be the SM-like Higgs boson, while Point 2 depicts a solution in which h_2 behaves to be SM-like, while $m_{h_1} \sim 28$ GeV. In the latter case, the other Higgs bosons are realized heavier than about 100 GeV. We explore further to see if such backgrounds can be probed in the light of the excess observed in the dimuon processes with $m_{\mu\mu} \sim 28$ GeV. If the light Higgs bosons (A -boson if h_1 is SM-like or h_1 if h_2 is SM-like) are not included, the predictions of LS-2HDM overlap with the SM background, while the contributions from the light Higgs bosons can count for the excess. We find similar results from the analyses over both cases.

Acknowledgment

CSU would like to thank the Physics and Astronomy Department and Bartol Research Institute of the University of Delaware, for kind hospitality where part of this work has been done. Part of the calculations reported in this paper were performed at the National Academic Network and Information Center (ULAKBIM) of TUBITAK, High Performance and Grid Computing Center (TRUBA Resources).

References

- [1] G. Aad *et al.* [ATLAS Collaboration], Phys. Lett. B **716**, 1 (2012) [arXiv:1207.7214 [hep-ex]]. S. Chatrchyan *et al.* [CMS Collaboration], Phys. Lett. B **716**, 30 (2012) [arXiv:1207.7235 [hep-ex]].
- [2] The ATLAS collaboration [ATLAS Collaboration], ATLAS-CONF-2017-046; A. M. Sirunyan *et al.* [CMS Collaboration], JHEP **1711**, 047 (2017) doi:10.1007/JHEP11(2017)047 [arXiv:1706.09936 [hep-ex]].
- [3] The ATLAS collaboration [ATLAS Collaboration], ATLAS-CONF-2019-004.

- [4] The ATLAS collaboration [ATLAS Collaboration], ATLAS-CONF-2018-002.
- [5] V. Khachatryan *et al.* [CMS Collaboration], JHEP **1510**, 144 (2015) doi:10.1007/JHEP10(2015)144 [arXiv:1504.00936 [hep-ex]]; G. Aad *et al.* [ATLAS Collaboration], Phys. Rev. D **92**, no. 1, 012006 (2015) [arXiv:1412.2641 [hep-ex]]; G. Aad *et al.* [ATLAS Collaboration], JHEP **1508**, 137 (2015) [arXiv:1506.06641 [hep-ex]]; S. Chatrchyan *et al.* [CMS Collaboration], JHEP **1401**, 096 (2014) [arXiv:1312.1129 [hep-ex]].
- [6] A. M. Sirunyan *et al.* [CMS Collaboration], Phys. Rev. Lett. **120**, no. 7, 071802 (2018) [arXiv:1709.05543 [hep-ex]]; The ATLAS collaboration [ATLAS Collaboration], ATLAS-CONF-2017-047; The ATLAS collaboration [ATLAS Collaboration], ATLAS-CONF-2018-004.
- [7] A. M. Sirunyan *et al.* [CMS Collaboration], Phys. Rev. Lett. **121**, no. 12, 121801 (2018) doi:10.1103/PhysRevLett.121.121801 [arXiv:1808.08242 [hep-ex]].
- [8] See, for instance,
G. Aad *et al.* [ATLAS Collaboration], arXiv:1907.02749 [hep-ex]; The ATLAS collaboration [ATLAS Collaboration], ATLAS-CONF-2019-010; CMS Collaboration [CMS Collaboration], CMS-PAS-HIG-17-033; CMS Collaboration [CMS Collaboration], CMS-PAS-HIG-18-023; A. M. Sirunyan *et al.* [CMS Collaboration], Eur. Phys. J. C **79**, 564 (2019) [arXiv:1903.00941 [hep-ex]]. A. M. Sirunyan *et al.* [CMS Collaboration], arXiv:1905.07453 [hep-ex]; CMS Collaboration [CMS Collaboration], CMS-PAS-HIG-18-020;
- [9] A. M. Sirunyan *et al.* [CMS Collaboration], JHEP **1811**, 161 (2018) [arXiv:1808.01890 [hep-ex]]; A. M. Sirunyan *et al.* [CMS Collaboration], JHEP **1711**, 010 (2017) [arXiv:1707.07283 [hep-ex]].
- [10] P. Ko, J. Li and C. Yu, arXiv:1610.07526 [hep-ph]; K. Lane and L. Pritchett, arXiv:1701.07376 [hep-ph].
- [11] S. I. Godunov, V. A. Novikov, M. I. Vysotsky and E. V. Zhemchugov, arXiv:1808.02431 [hep-ph]; K. Lane and L. Pritchett, arXiv:1701.07376 [hep-ph]; P. Ko, J. Li and C. Yu, arXiv:1610.07526 [hep-ph]; J. Bernon, J. F. Gunion, Y. Jiang and S. Kraml, Phys. Rev. D **91**, no. 7, 075019 (2015) [arXiv:1412.3385 [hep-ph]].
- [12] For recent reviews, see
G. Bhattacharyya and D. Das, Pramana **87**, no. 3, 40 (2016) [arXiv:1507.06424 [hep-ph]];
- [13] R. Aggleton, D. Barducci, N. E. Bomark, S. Moretti and C. Shepherd-Themistocleous, JHEP **1702**, 035 (2017) [arXiv:1609.06089 [hep-ph]];
- [14] E. J. Chun, S. Dwivedi, T. Mondal, B. Mukhopadhyaya and S. K. Rai, Phys. Rev. D **98**, no. 7, 075008 (2018) [arXiv:1807.05379 [hep-ph]].
- [15] See, for instance,
F. Mahmoudi, S. Neshatpour and J. Orloff, JHEP **1208**, 092 (2012) [arXiv:1205.1845 [hep-ph]]; A. Arbey, M. Battaglia, F. Mahmoudi and D. Martinez Santos, Phys. Rev.

- D **87**, no. 3, 035026 (2013) [arXiv:1212.4887 [hep-ph]]; B. Nis, A. Cici, Z. Kirca and C. S. Un, arXiv:1702.04185 [hep-ph]; P. Arnan, D. Beirevi, F. Mescia and O. Sumensari, Eur. Phys. J. C **77**, no. 11, 796 (2017) [arXiv:1703.03426 [hep-ph]].
- [16] C. Bobeth, M. Gorbahn, T. Hermann, M. Misiak, E. Stamou and M. Steinhauser, Phys. Rev. Lett. **112**, 101801 (2014) [arXiv:1311.0903 [hep-ph]]; C. Bobeth, M. Gorbahn and E. Stamou, Phys. Rev. D **89**, no. 3, 034023 (2014) [arXiv:1311.1348 [hep-ph]]; T. Hermann, M. Misiak and M. Steinhauser, JHEP **1312**, 097 (2013) [arXiv:1311.1347 [hep-ph]].
- [17] R. Aaij *et al.* [LHCb Collaboration], Phys. Rev. Lett. **110**, no. 2, 021801 (2013) [arXiv:1211.2674 [hep-ex]]; Y. Amhis *et al.* [Heavy Flavor Averaging Group Collaboration], arXiv:1207.1158 [hep-ex].
- [18] P. Ko, Y. Omura and C. Yu, Phys. Lett. B **717**, 202 (2012) [arXiv:1204.4588 [hep-ph]]; T. Nomura and P. Sanyal, arXiv:1907.02718 [hep-ph].
- [19] T. D. Lee, Phys. Rev. D **8**, 1226 (1973). doi:10.1103/PhysRevD.8.1226
- [20] R. D. Peccei and H. R. Quinn, Phys. Rev. D **16**, 1791 (1977); R. D. Peccei and H. R. Quinn, Phys. Rev. Lett. **38**, 1440 (1977).
- [21] N. Turok and J. Zadrozny, Nucl. Phys. B **358** (1991) 471; M. Joyce, T. Prokopec, and N. Turok, Phys. Rev. D **53** (1996) 2958 [hep-ph/9410282]; K. Funakubo, A. Kakuto, and K. Takenaga, Prog. Theor. Phys. **91** (1994) 341 [hep-ph/9310267]; A. T. Davies, C. D. Froggatt, G. Jenkins, and R. G. Moorhouse, Phys. Lett. B **336** (1994) 464; J. M. Cline, K. Kainulainen, and A. P. Vischer, Phys. Rev. D **54** (1996) 2451 [hep-ph/9506284]; J. M. Cline and P.-A. Lemieux, Phys. Rev. D **55** (1997) 3873 [hep-ph/9609240]; M. Laine and K. Rummukainen, Nucl. Phys. B **597** (2001) 23 [hep-lat/0009025]; L. Fromme, S. J. Huber, and M. Seniuch, JHEP **0611** (2006) 038 [hep-ph/0605242]; G. C. Dorsch, S. J. Huber and J. M. No, JHEP **1310**, 029 (2013) [arXiv:1305.6610 [hep-ph]].
- [22] S. R. Choudhury and N. Gaur, Phys. Lett. B **451**, 86 (1999) [hep-ph/9810307]; K. S. Babu and C. F. Kolda, Phys. Rev. Lett. **84**, 228 (2000) [hep-ph/9909476].
- [23] G. Buchalla, A. J. Buras and M. E. Lautenbacher, Rev. Mod. Phys. **68**, 1125 (1996) [hep-ph/9512380].
- [24] J. F. Gunion and H. E. Haber, Phys. Rev. D **67**, 075019 (2003) [hep-ph/0207010].
- [25] See, for instance,
G. C. Branco, P. M. Ferreira, L. Lavoura, M. N. Rebelo, M. Sher and J. P. Silva, Phys. Rept. **516**, 1 (2012) [arXiv:1106.0034 [hep-ph]]; R. A. Diaz, hep-ph/0212237; I. Chakraborty and A. Kundu, Phys. Rev. D **92**, no. 9, 095023 (2015) [arXiv:1508.00702 [hep-ph]]; F. Mahmoudi and O. Stal, Phys. Rev. D **81**, 035016 (2010) [arXiv:0907.1791 [hep-ph]]; I. P. Ivanov and J. P. Silva, Phys. Rev. D **92**, no. 5, 055017 (2015) [arXiv:1507.05100 [hep-ph]].
- [26] K. A. Olive *et al.* [Particle Data Group], Chin. Phys. C **38**, 090001 (2014). doi:10.1088/1674-1137/38/9/090001

- [27] Porod, W. *Comput. Phys. Commun.* **2003**, 153, 275.
- [28] Porod, W. and Staub, F. *Comput. Phys. Commun.* **2012** 183, 2458.
- [29] Staub, F. **2008**, *Preprint arXiv:0806.0538*.
- [30] Staub, F. *Comput. Phys. Commun.* **2011** 182, 808.
- [31] J. Alwall, M. Herquet, F. Maltoni, O. Mattelaer and T. Stelzer, *JHEP* **1106**, 128 (2011) doi:10.1007/JHEP06(2011)128 [arXiv:1106.0522 [hep-ph]].
- [32] A. M. Sirunyan *et al.* [CMS Collaboration], *Phys. Lett. B* **793**, 320 (2019) doi:10.1016/j.physletb.2019.03.064 [arXiv:1811.08459 [hep-ex]].
- [33] For an incomplete list, see
P. M. Ferreira, R. Santos, H. E. Haber and J. P. Silva, *Phys. Rev. D* **87**, 055009 (2013) [arXiv:1211.3131 [hep-ph]]; T. Han, T. Li, S. Su and L. T. Wang, *JHEP* **1311**, 053 (2013) [arXiv:1306.3229 [hep-ph]]; J. Ke, H. Luo, M. x. Luo, K. Wang, L. Wang and G. Zhu, *Phys. Lett. B* **723**, 113 (2013) [arXiv:1211.2427 [hep-ph]]; W. Abdallah, A. Hammad, S. Khalil and S. Moretti, *Phys. Rev. D* **95**, no. 5, 055019 (2017) [arXiv:1608.07500 [hep-ph]]; A. Hammad, S. Khalil and S. Moretti, *Phys. Rev. D* **93**, no. 11, 115035 (2016) [arXiv:1601.07934 [hep-ph]]; S. Khalil and S. Moretti, arXiv:1510.05934 [hep-ex]; A. Hammad, S. Khalil and S. Moretti, *Phys. Rev. D* **92**, no. 9, 095008 (2015) [arXiv:1503.05408 [hep-ph]]; W. Abdallah, S. Khalil and S. Moretti, *Phys. Rev. D* **91**, no. 1, 014001 (2015) [arXiv:1409.7837 [hep-ph]]. M. Hemed, S. Khalil and S. Moretti, *Phys. Rev. D* **89**, no. 1, 011701 (2014) [arXiv:1312.2504 [hep-ph]]; C. S. Un and O. Ozdal, *Phys. Rev. D* **93**, 055024 (2016) [arXiv:1601.02494 [hep-ph]];
- [34] Zafer Altın, Ali Çiçi, Zerrin Kırca, Qaisar Shafi and Cem Salih Ün, “Gluino Search with Stop and Top in NUGM at LHC and Future Colliders” (in preparation).